# Debye Brownian oscillator and Debye-type noise: A series solution versus Monte Carlo simulation

Qian Qiu and Jing-Dong Bao*
*Department of Physics, Beijing Normal University, Beijing 100875, People's Republic of China*

(Received 22 January 2021; revised 16 May 2021; accepted 21 June 2021; published 13 July 2021)

For the Debye Brownian oscillator, we present a series solution to the generalized Langevin equation describing the motion of a particle. The external potential is considered to be a harmonic potential and the spectral density of driven noise is a hard cutoff at high finite frequencies. The results are in agreement with both numerical calculations and Monte Carlo simulations. We demonstrate abnormal weak ergodic breaking; specifically, the long-time average of the observable vanishes but the corresponding ensemble average continues to oscillate with time. This Debye Brownian oscillator does not arrive at an equilibrium state and undergoes underdamped-like motion for any model parameter. Nevertheless, ergodic behavior and equilibrium can be recovered concurrently using a strong bound potential. We give an understanding of the behavior as being the consequence of discrete breather modes in the lattices similar to the formation of an additional periodic signal. Furthermore, we compare the results calculated by cutting off separately the spectral density and the correlation function of colored noise.

DOI: 10.1103/PhysRevE.104.014114

## I. INTRODUCTION

The well-known Debye theory in condensed matter was established initially to study the heat capacity of metallic materials [1–3]. Because lattice vibrational modes in the crystal are limited in actual systems, the theory simplifies the frequency distribution of phonons in the crystals; specifically, the high frequencies are cut off at an appropriate frequency $\omega_s$, called the Debye frequency [3]. The theory has widely been used in equilibrium statistical situations, for instance, molecular magnets [4], thermal conductance of materials [5], glasses [6–9], and crystals [10–12]. Brownian dynamics associated with the generalized Langevin equation (GLE) was also shown to emerge from an open Hamiltonian system of a particle in a bath potential [13]. Any realistic spectral density for noise decays at large frequencies because physical quantities should seemingly not diverge [14]. Moreover, the Brownian limit for the GLE may not be a justifiable approximation for collisions with a pure solid. If $\omega_s$ is large, the memory function in the GLE is represented by a Dirac $\delta$ function and therefore the corresponding noise reduces to white noise. The Debye frequency cutoff affects the properties of the system significantly. For example, the dissipative dynamics models usually assume a particle is coupled weakly to a heat bath, in which the frequency distribution of oscillators needs to be cut at high frequencies. However, an improper selection of the Debye frequency may lead to a negative specific quantity [15]. A focus on the dynamic effect arising from the choice of the Debye frequency cutoff is required in noise-driven stochastic processes.

In practice, the absence of some frequencies may lead to nonstationary calculated results of an observable; therefore, the question arises: Can a bounded potential make the particle subjected to such colored noise approach an equilibrium state? In particular, does a nonlinear Debye Brownian oscillator (DBO) reveal ergodic behavior? As is well known, the ergodic hypothesis states that the long-time average of an observable $\bar{O}(t)$, $\lim_{t\to\infty}\bar{O}(t) = t^{-1}\int_0^t O(t')dt'$, and the ensemble average $\langle O\rangle$ are identical [16]. However, ergodicity should be broken in some complex structures such as glass, supercooled liquids, Lorentz gases, and laser-cooled atoms [17–22]. For many-body systems that need times too long to observe the ergodic behavior, the time average of an observable is difficulty to establish. This kind of weak ergodicity breaking has been illustrated in Refs. [23,24], in which the ensemble average of the observable is assumed to be stationary and equals zero as long as a symmetric bounded potential is added to the system.

In essence, our approach is a fusion of Zwanzig's work with the theory of generalized Brownian motion [13]. This allows us to easily treat lattices dynamics at finite temperature using the methods of stochastic theory. Our finding departs from the available ergodicity breakdown in one fundamental way. We augment the standard conditions with ideas related to the Khinchin theorem [25,26] for generalized Brownian motion, which states that an observable is ergodic if its associated correlation function is irreversible. Note that a precondition needs to be assumed; specifically, the process must be stationary. A corollary arises—a nonstationary process leads to the breakdown of ergodicity. The DBO possesses an opposite averaging behavior in comparison with the usual averaging behavior; expressly, its long-time mean position vanishes but the corresponding ensemble average continues oscillating with time.

In this paper, we focus on nonergodic behaviors of the DBO. The concern regarding the position of the particle arises because with current technology individual molecules can now be tracked with exquisite precision. We use a series expansion to obtain an analytic solution of the linear GLE driven by a Debye-type colored noise. However, the Laplace

*jdbao@bnu.edu.cn

 

transform technique [27] encounters a mathematical dilemma [28–30] because the Laplace transform of the response function has an infinite number of singularities in the complex plane. The dynamics of a particle subject to a nonlinear bound potential and Debye-type colored noise (i.e., a nonlinear DBO) is simulated. We demonstrate that the ergodic behavior of the system can be recovered by introducing a strong bounded potential. We reveal abnormal weak ergodic breaking and compare two different types of truncation for the noise spectral density (NSD) and the noise correlation function. Finally, in Appendix A, we propose an equivalent model in which white noise combined with a periodic driving force is treated to simplify the Debye treatment.

## II. DBO AND ITS SERIES SOLUTION

The generalized Brownian motion of a particle with mass $m$ in a potential $U(x)$ is described by the following GLE [31]:

$$m\dot{v}(t) = -m\int_0^t \Gamma(t-t_1)v(t_1)dt_1 - U'(x) + F(t), \tag{1}$$

where $\Gamma(t)$ is the memory function and $F(t)$ is the random force of zero mean; their relationship underscores the fluctuation-dissipation theorem: $C_F(t) \equiv \langle F(t)F(0)\rangle = mk_BT\Gamma(t)$. Here, $k_B$ denotes the Boltzmann constant, $T$ the temperature, and $\langle\ldots\rangle$ the ensemble average. In the GLE formalism, the NSD associated with the Debye model has the following form:

$$\rho(\omega) = \begin{cases} \frac{3\gamma^2}{\omega_s^3}, & \omega \leqslant \omega_s; \\ 0, & \text{otherwise}, \end{cases} \tag{2}$$

where $\gamma$ denotes a constant which determines the strength of the friction [32,33]. Consequently, the memory function $\Gamma(t)$ appearing in the GLE is given by $\Gamma(t) = 3\gamma^2\omega_s^{-3}\sin(\omega_s t)t^{-1}$.

The DBO is associated with a particle moving in a harmonic potential $U(x) = \frac{1}{2}m\Omega^2x^2$. The formal solution of the GLE reads $v(t) = h(t)v(0) - \Omega^2H(t)x(0) + \frac{1}{m}\int_0^t h(t-t')F(t')dt'$ and $x(t) = G(t)x(0) + H(t)v(0) + \frac{1}{m}\int_0^t H(t-t')F(t')dt'$, where $G(t) = 1 - \Omega^2\int_0^t H(t')dt'$ and $H(t) = \int_0^t h(t')dt'$, in which $H(t)$ and $h(t)$ are two response functions [34]. Assuming $\langle F(t)O(0)\rangle = 0$ $(O = x, v)$, and $\langle x(t)v(0)\rangle = \langle v(t)x(0)\rangle = 0$, we have $h(t) = \langle v(t)v(0)\rangle/\langle v^2(0)\rangle = C_v(t)$ as well as $G(t) = \langle x(t)x(0)\rangle/\langle x^2(0)\rangle = C_x(t)$.

No closed form has been found for the time domain function in Eq. (1) with Eq. (2). They can, however, be evaluated accurately using numerical methods. For a linear GLE, we use the initial velocity $v(0)$ to multiply Eq. (1) and perform the ensemble average. The integral-differential equation for the velocity autocorrelation function is given by

$$m\frac{dC_v(t)}{dt} = -m\int_0^t [\Gamma(t_1) + \Omega^2]C_v(t-t_1)dt_1. \tag{3}$$

Because the velocity autocorrelation function must be an even function of time [35], we expand $C_v(t)$ as a series that includes only the even powers of $t$, i.e.,

$$C_v(t) = \sum_{n=0}^{\infty} a_n t^{2n}. \tag{4}$$

The same treatment for the memory function $\Gamma(t)$ also applies:

$$\Gamma(t) = \sum_{l=0}^{\infty} b_l t^{2l}. \tag{5}$$

For the left-hand side of Eq. (3), we have

$$\frac{dC_v(t)}{dt} = \sum_{n=0}^{\infty} 2na_n t^{2n-1}, \tag{6}$$

and the memory friction yields

$$\begin{aligned} &-m\int_0^t \Gamma(t_1)C_v(t-t_1)dt_1 \\ &= -\int_0^t \sum_{l=0}^{\infty} b_l t_1^{2l} \sum_{n=0}^{\infty} a_n(t-t_1)^{2n}dt_1. \end{aligned} \tag{7}$$

Simplifying and completing the above integral yields

$$\begin{aligned} &-m\int_0^t \Gamma(t_1)C_v(t-t_1)dt_1 \\ &= -\sum_{n=0}^{\infty}\sum_{l=0}^{\infty} \frac{2n!\,2l!}{(2n+2l+1)!}a_n b_l t^{2(n+l)}. \end{aligned} \tag{8}$$

Substituting Eqs. (6) and (8) into Eq. (3) produces a recurrence relation for $a_n$:

$$a_n = \sum_{l=0}^{n-1} \frac{[2(n-l-1)]!\,2l!}{(2n)!}a_{n-l-1}b_l. \tag{9}$$

The memory function $\Gamma(t)$ can be expanded as a series, $\Gamma(t) = \frac{3\gamma^2}{\omega_s^3}\sum_{l=0}^{\infty}\frac{(-1)^l\omega_s^{2l+1}}{(2l+1)!}t^{2l}$. Accordingly, in Eq. (7),

$$b_l = \frac{3\gamma^2(-1)^l\omega_s^{2(l-1)}}{(2l+1)!}. \tag{10}$$

In the absence of a potential, we obtain expressions for the coefficients of the series solution for $C_v(t)$:

$$a_n = 3\gamma^2\sum_{l=0}^{n-1}(-1)^{l+1}(\omega_s)^{2(l-1)}\frac{[2(n-l-1)]!}{(2l+1)(2n)!}a_{n-l-1}. \tag{11}$$

Taking into account the harmonic potential in Eq. (3), each coefficient $a_n$ is determined as

$$\begin{aligned} a_n = {} & 3\gamma^2\sum_{l=0}^{n-1}(-1)^{l+1}(\omega_s)^{2(l-1)}\frac{[2(n-l-1)]!}{(2l+1)(2n)!}a_{n-l-1} \\ & - \frac{\Omega^2}{2n(2n+1)}a_{n-1}. \end{aligned} \tag{12}$$

As long as $C_v(t)$ is known, and using the relation between $h(t)$ and $G(t)$, the final series solution of $C_x(t)$ becomes

$$C_x(t) = 1 - \Omega^2\sum_{n=0}^{\infty}\frac{a_n}{(2n+1)(2n+2)}t^{2n+2}. \tag{13}$$

Furthermore, with $C_x(t)$ and $C_v(t)$, the first and second moments of the position and velocity of the DBO may be established.

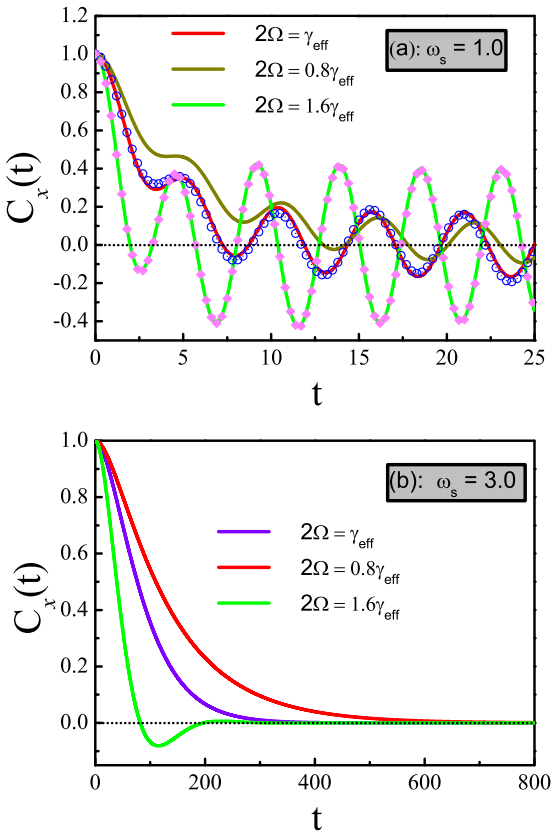


FIG. 1. Time-dependent position autocorrelation function of the DBO for (a) small Debye frequency ($\omega_s = 1.0$) and (b) large Debye frequency ($\omega_s = 3.0$). The curves in (a) are the series solution. Blue circles in (a) are obtained from Monte Carlo simulations for Eq. (1), and pink diamonds mark results obtained from numerical integral calculations of Eq. (3). The curves in (b) are also obtained from numerical integral calculations of Eq. (3). The parameters used are $\gamma = 0.5$, $k_BT = 1$, and $m = 1$.

In Fig. 1, we plot the series solution obtained and compare the results of Monte Carlo simulations; here the algorithm used was developed by one of us in Ref. [36]. Details of the simulations are given in Appendix B. Clearly, the results obtained from the series solution and the Monte Carlo calculations agree well.

## III. ABNORMAL NONERGODIC BEHAVIOR

The analysis concerning whether the DBO is ergodic is straightforward. For the motion of a particle in a bounded potential, the ensemble average of the position in an equilibrium state is determined from $\langle x\rangle_{\rm eq} = \int_{-\infty}^{\infty} xP_{\rm eq}(x)dx$, where $P_{\rm eq}(x) = Z^{-1}\exp[-U(x)/k_BT]$ is the Boltzmann distribution and $Z$ is the partition function. With a harmonic potential symmetric about the origin of the coordinate, $\langle x\rangle_{\rm eq}$ is equal to zero in theory. However, from the calculation of $C_x(t)$ and $C_v(t)$, we know that the time-dependent $\langle x(t)\rangle$ should not vanish in the long-time limit.

Figure 2 shows more direct evidence with results calculated from Monte Carlo simulations of $\langle x(t)\rangle$. In conclusion, the DBO cannot reach an equilibrium state when the Debye frequency $\omega_s$ has a finite value; this is indeed a kind of

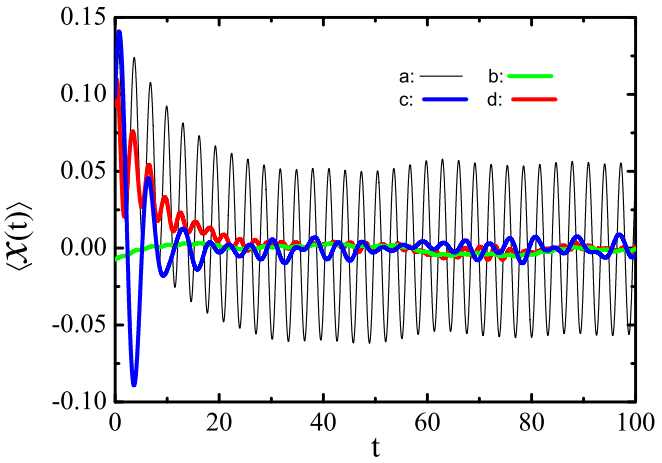


FIG. 2. Time-dependent ensemble average of the position calculated in Monte Carlo simulations with $10^5$ trajectories. Curve (a): $\langle x(t)\rangle$ of DBO with $\omega_s = 0.5$ and $\Omega^2 = 1.0$. The initial condition sets $\langle x(0)\rangle = 0.1$ and $\langle v(0)\rangle = 0.1$. Curve (b): The same as curve (a), except the initial condition is set to $\langle x(0)\rangle = 0$ and $\langle v(0)\rangle = 0$. Curve (c): Also the same as curve (a), but with Debye frequency of $\omega_s = 1.5$. Curve (d): $\langle x(t)\rangle$ of the particle subjected to Debye-type noise and quartic potential $U(x) = \frac{1}{4}x^4$; the parameters and initial conditions are the same as for curve (a). All other parameters for the curves are set identically, i.e., $\gamma = 0.5$, $k_BT = 1$, and $m = 1$.

nonergodicity. Nevertheless, the time average of the DBO's position $\bar{x}(t)$ is not easy to calculate theoretically; we also used the Monte Carlo method to evaluate this quantity. The results are plotted in Fig. 3.

Upon inspection, we find a prominent result—$\bar{x}(t)$ converges to zero in the long-time limit; however, it is clear that $\lim_{t\to\infty}\langle x(t)\rangle \neq 0$. That is, the DBO is indeed nonergodic. This kind of nonergodicity is different from other types that have been widely studied; specifically, the former may not equal zero but the latter vanishes. From the Khinchin theorem, we know that a dynamical variable is nonergodic if its auto-

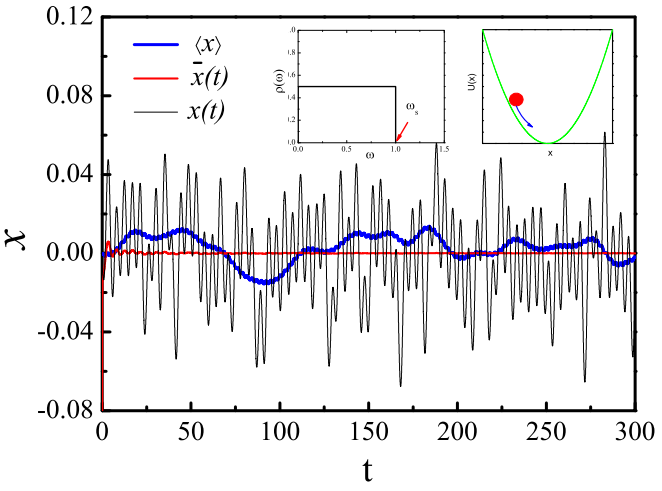


FIG. 3. A trajectory of the DBO with $\Omega = 1.0$ and its time (red line) and ensemble (blue line) averages. The parameters used are $\omega_s = 0.4$, $\gamma = 0.5$, $k_BT = 1$, and $m = 1$. The two insets plot the Debye-type noise spectrum and the harmonic potential.

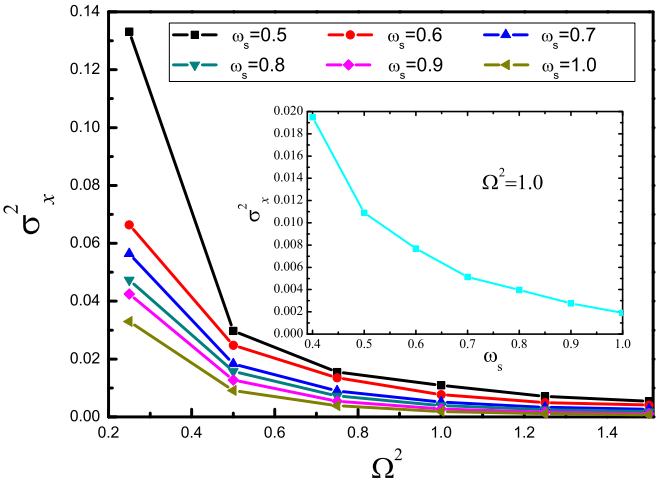


FIG. 4. Steady variance of position $\sigma_x^2$ as functions of $\Omega^2$ and (inset) $\omega_s$. Data are from Monte Carlo simulation with 50 000 trajectories. The parameter settings are $m = 1$, $k_BT = 1$, and $\gamma = 0.5$.

correlation function or response function is not equal to zero in the long-time limit [25,26]. This theorem requires that the process studied must be stationary. Ergodic breakdown arises from the vanishing of the effective Markovian friction. Here we focus on a physical system with autocorrelation functions of velocity and position oscillating with time and reveal an abnormal type of weak ergodicity breaking.

To investigate the influences of both the Debye frequency $\omega_s$ and the potential frequency $\Omega^2$ on the nonergodic behavior of the system, we use variance $\sigma_A^2$ of dynamical quantity $A$ to measure the degree of ergodic breaking. Defined as $\sigma_A^2(t) \equiv \langle(\bar{A}(t) - \langle\bar{A}(t)\rangle)^2\rangle$, then dynamical quantity $A$ is ergodic if $\sigma_A^2(t) \to 0$ as $t \to \infty$ [23,24,37]. With $A$ replaced by the DBO's coordinate $x(t)$, we apply the usual theory for a stochastic process [38] and compute the quantity

$$\sigma_x^2(t) = \frac{1}{t^2}\int_0^t dt_2 \int_0^t dt_1[\langle x(t_2)x(t_1)\rangle - \langle x(t_1)\rangle\langle x(t_2)\rangle]. \tag{14}$$

In Fig. 4, we show the steady variance of the position for the DBO. The DBO reveals a kind of ergodicity breaking. With increasing $\omega_s$, the value of $\sigma_x^2$ decreases and approaches zero. This indicates that the DBO reduces to an ordinary Brownian oscillator for large $\omega_s$. Moreover, the memory function $\Gamma(t)$ approaches the Dirac $\delta$ function and therefore the associated noise becomes white noise. We also find that the strong bound of the potential is beneficial for ergodicity; the larger $\omega_s$ is, the smaller $\Omega$ can be chosen to ensure $\sigma_x^2$ vanishes. To investigate recovery for a Debye-type noise-driven particle, we now consider a symmetric strong bounded potential $U(x) = \frac{1}{4}x^4$. A common assumption is that $\omega_s$ is sufficiently large if $\omega_s \gg U''(x_{\min})$ [39–41]. For this potential, $U''(x_{\min}) = 0$. In addition, the linear response no longer holds when the potential is strongly bound and no analytic expression for $C_x(t)$ can be determined. As expected, the particle arrives at an equilibrium state although the NSD is still cut off at finite high frequency [Fig. 2, curve (d)], indicating that the nonergodic behavior is independent of the quadratic nature of the potential.

## IV. ABNORMAL UNDERDAMPING BEHAVIOR

Because nonstationary properties create ergodicity breakdown, damping of the DBO is found to vary. The usual damping oscillator of Newtonian dynamics has two distinct regimes: underdamping for which $x(t)$ oscillates and crosses the coordinate axis and overdamping for which $x(t)$ decays monotonically with time to zero. Similarly, when $C_x(t)$ starts from unity and is positive at late times, the system exhibits overdamped behavior. When $C_x(t)$ displays a nonmonotonic variation and crosses the coordinate axis, the system is said to undergo an underdamped behavior but differs from the usual Brownian oscillator [42].

For a non-Markovian process described by the GLE, the effective friction strength is defined as $\gamma_{\text{eff}} = \int_0^\infty \Gamma(t)dt$. For the DBO studied, the effective friction strength is given by $\gamma_{\text{eff}} = \frac{3\pi\gamma^2}{2\omega_s^3}$. That is, with increasing $\omega_s$, the effective friction strength decreases, and the attenuation rate of oscillation slows. Figure 5(a) reveals clearly this interesting phenomenon. A transition is observed from overdamped to underdamped behavior with respect to $\gamma_{\text{eff}}$ and $\Omega$ when $\omega_s$ is large [Fig. 1(b)]. As for a typical damped system, $\gamma_{\text{eff}} = 2\Omega$ is the critical point. For the usual dynamics, condition $\gamma_{\text{eff}} > 2\Omega$ corresponds to overdamping and $\gamma_{\text{eff}} < 2\Omega$ to underdamping. However, the DBO for small $\omega_s$ undergoes a transition from overdamped to underdamped behavior [Fig. 1(a)]. Obviously, the effective damping of the system is to be monotonic for small $\omega_s$. The position autocorrelation function $C_x(t)$ is always a nonmonotonic function of time for large or small $\Omega$. More importantly, if the chosen Debye frequency is too small, the amplitude of $C_x(t)$ decays rapidly and approaches a constant [Fig. 5(b)].

The dependence of the result on the potential frequency $\Omega$ is plotted in Fig. 5(c). As $\Omega$ increases, the amplitude of $C_x(t)$ increases in contrast to $\sigma_x$. However, the oscillation of the DBO decreases with increasing $\Omega$. In the extreme case, the impact of driven noise should become minimal; therefore, the role of the harmonic potential is expected to dominate the particle dynamics, and then the situation becomes deterministic. There is then no difference between $\langle\bar{x}\rangle$ and $\bar{x}$, but the amplitude of the DBO strengthens with increasing $\Omega$. Combining the current phenomenon with the previous definition, we find that the DBO enters an underdamped-like regime if $\omega_s$ is small. Specifically, insufficient energy dissipation between the DBO and the environment leads to the former becoming stationary, and the presence of the harmonic potential strengthens the oscillation. Hence, this kind of abnormal damping originates with the DBO unable to become stationary because high frequencies are not cut off.

Our results have demonstrated that Debye-type colored noise does not induce nonergodic behavior in the particle for a nonlinear bounded potential; however, the transient-to-equilibrium behavior changes. Here we consider a bistable potential, $U(x) = \frac{1}{4}x^4 - \frac{1}{2}x^2$. The potential has two local minima and one local maximum. Initially, test particles are set in one of the wells and then undergo diffusion between the two wells.

In Fig. 6, we use the ratio $N_L/N_0$ to indicate transient behavior, where $N_L$ is the number of test particles in the left trap and $N_0$ is the total number of test particles. We note that the

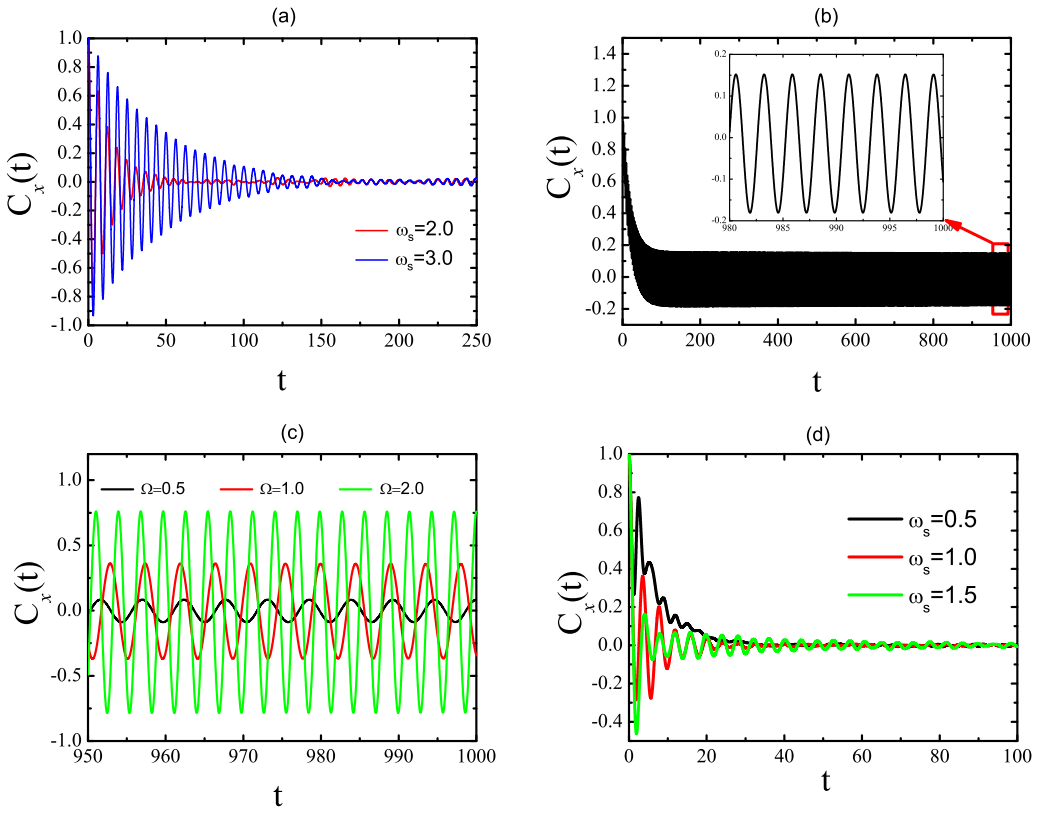


FIG. 5. Time-dependent position autocorrelation function of a DBO at fixed $\gamma = 0.5$. (a) Fixed potential parameter $\Omega^2 = 1.0$ and two Debye frequencies $\omega_s = 2.0$ and 3.0 are used. (b) Small Debye frequency of $\omega_s = 0.4$ and $\Omega^2 = 1.0$. The inset is a detail from its large time behavior. (c) Fixed Debye frequency $\omega_s = 1.0$ and harmonic potential frequencies $\Omega^2 = 0.25$, 1.0, and 4.0. The curves are calculated results obtained using the numerical integral, Eq. (3). (d) Position autocorrelation function of a particle in a quartic potential with Debye-type noise. The curves were obtained from Monte Carlo simulations. The Debye frequencies chosen are $\omega_s = 0.5$, 1.0, and 1.5.

cutoff for the NSD alters the transition behavior in two ways; specifically, the relaxation time is prolonged or the fluctuation is enhanced. This again shows that the truncation of the NSD induces nonstationarity.

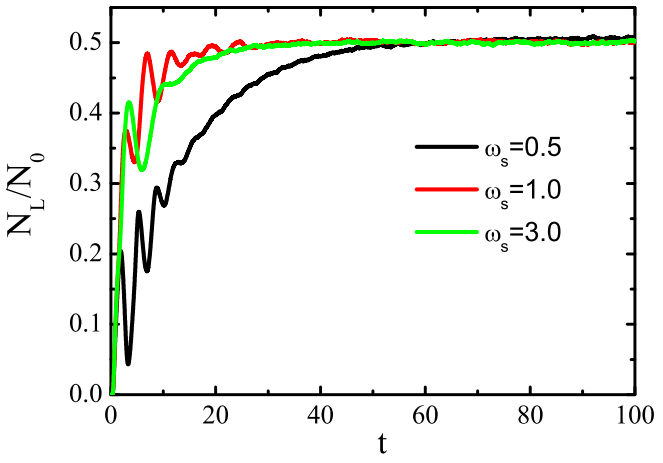


FIG. 6. Proportion of test particles in the left trap for simulating a nonlinear DBO. The data are calculated in Monte Carlo simulations with 50 000 test particles. The parameter settings are $m = 1$, $k_BT = 1$, and $\gamma = 0.5$; the Debye frequency used appears in the figure.

## V. ANOTHER TRUNCATION SCHEME: CUTOFF OF THE NOISE CORRELATION FUNCTION

Truncating the noise correlation function is an alternative method used [43,44]. In practice, the correlation time for noise is always finite, implying that a cutoff may be necessary for this function. Given the correlation for white noise is a $\delta$ function, we turn our attention to Ornstein-Uhlenbeck (OU) colored noise; its correlation function is $C_F(t) = \frac{D}{\tau_0} e^{-\frac{t}{\tau_0}}$ [45]. After a cutoff in $C_F(t)$ at large $t_c$, i.e.,

$$\Gamma(t) = Ae^{-\frac{t}{\tau_0}}\Theta(t - t_c), \tag{15}$$

we find the NSD of such noise from the Fourier transform,

$$\rho(\omega) = \frac{D}{(\omega\tau_0)^2 + 1}\left[\omega\tau_0 e^{-\frac{t_c}{\tau_0}} \sin(\omega t_c) - e^{-\frac{t_c}{\tau_0}} \cos(\omega t_c) + 1\right], \tag{16}$$

where $A$ is a constant and $\Theta(t)$ denotes the step function.

Correspondingly, we establish a cutoff in the NSD for OU noise at $\omega_s$; that is,

$$\rho(\omega) = \begin{cases} \frac{D}{(\omega\tau_0)^2+1}, & \omega \leqslant \omega_s; \\ 0, & \omega > \omega_s. \end{cases} \tag{17}$$

After truncation for these two schemes, we use the resulting noise to drive a Brownian particle moving in a harmonic potential.

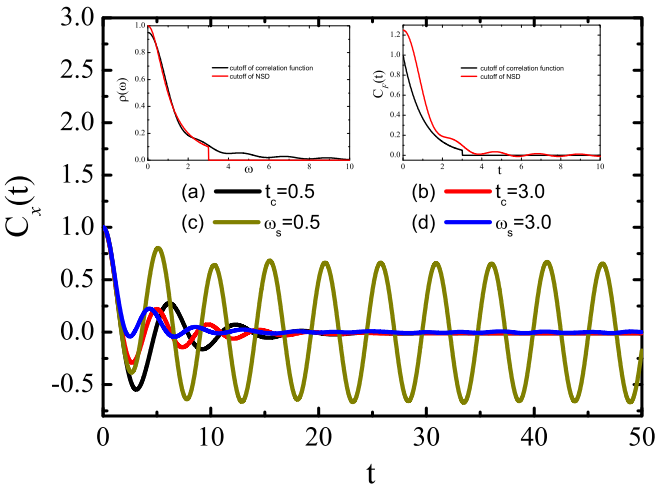


FIG. 7. Position autocorrelation function $C_x(t)$. Curves (a) and (b) are instances with a cutoff for the correlative function and NSD as in Eq. (16). The data are derived from numerical calculations of Eq. (3). Curves (c) and (d) are instances with a cutoff for the NSD, i.e., Eq. (17). The data are developed from Monte Carlo simulations. Parameter settings related to the truncations are indicated. Other parameter settings are $m = 1$, $k_BT = 1$, $D = 1$, and $\tau_0 = 1$. The insets are plots of the NSD and the correlation function of noise with frequency cutoffs.

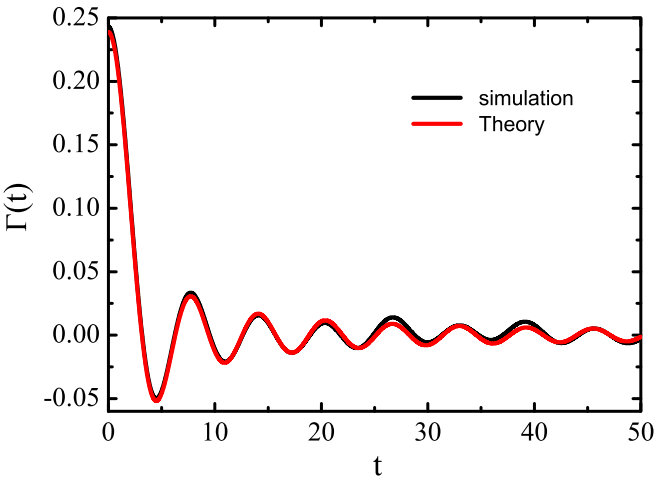


FIG. 8. Correlation function of Debye-type colored noise. The black line signifies Monte Carlo simulation data; the red line signifies theoretical values. The parameters used are set to $\omega_s = 1.0$, $\gamma = 0.5$, and $N = 2^{17}$.

Figure 7 shows the position autocorrelation function $C_x(t)$ calculated using these two treatments. The difference between the two types of truncation is significant. With a correlation function cutoff, the parameter $t_c$ only affects the relaxation time but not the ergodic behavior. However, with an OU noise cutoff, the NSD is similar to the Debye-type colored noise. In addition, abnormal nonergodic behavior occurs again when $\omega_s$ is small. Although the cutoff for the correlation function changes the NSD, the NSD is still smooth and the high frequencies are retained. Hence, ergodic behavior holds. This further proves that the cutoff at high frequencies generates the instability and ergodic breakdown.

## VI. SUMMARY

We have presented a series solution to the DBO described by the generalized Langevin equation. An algorithm simulating Debye-type colored noise with high finite-frequency cutoff was also developed. Our results have demonstrated that the DBO exhibits abnormal nonergodic behavior; specifically, the time average of observables vanishes in the long-time limit. However, the corresponding ensemble average continues to oscillate with time. This prominent result confirms that the system does arrive at an equilibrium state and undergoes underdamped-like motion for any model parameter settings. The nonstationary level of the observed quantities for the DBO is expected to decrease with increasing Debye frequency. By comparing the DBO with a nonlinear oscillator, we demonstrated that ergodic breakdown of the DBO arises from nonstationarity brought on by truncation, whereas the harmonic potential enhances this effect. This behavior is similar to forced vibration in lattices. That is, we understand this as a consequence of the discrete breather modes and similar to the formation of an additional periodic signal (see Appendix A).

Furthermore, our results for the cutoff of either the spectral density or the correlation function for OU noise suggest that abnormal nonergodic behavior is a general consequence of NSD truncation and does not depend on its specific form. Through studying the instability and nonergodic properties of the DBO, we have given a more comprehensive understanding of the influence of NSD truncation on driven stochastic processes, whereas previous studies have paid more attention to the absence of low frequencies [46]. One must be careful in treating the high frequency modes, ensuring a smooth decay rather than a hard cutoff. Of course, the Debye cutoff in frequency is still an effective way of dealing with divergences in strong nonlinear bounded potentials or when the cutoff frequency is set very large.

## ACKNOWLEDGMENTS

This work was supported by the National Natural Science Foundation of China under Grants No. 11735005 and No. 11790325.

## APPENDIX A: ALTERNATIVE UNDERSTANDING FOR PERSISTENT OSCILLATION

In substituting for the effect of Debye-type colored noise, we use a periodic signal $A\cos\Omega_0(t)$ to drive a Brownian particle in a harmonic potential. The Langevin equation for this Brownian oscillator reads

$$m\ddot{x} + \gamma\dot{x} + m\Omega^2 x = A\cos(\Omega_0 t) + \xi(t), \tag{A1}$$

and the position autocorrelation function satisfies

$$m\ddot{C}_x(t) + \gamma\dot{C}_x(t) + m\Omega^2 C_x(t) = A\cos(\Omega_0 t). \tag{A2}$$

The characteristic equation corresponding to Eq. (A2) is $ms^2 + \gamma s + m\Omega^2 = 0$. Its two roots are given by $s_{1,2} =$

$-\frac{\gamma}{2m} \pm a$, where $a = \sqrt{(\frac{\gamma}{m})^2 - 4\Omega^2}$. We then have

$$C_x(t) = \frac{1}{2a} e^{-\frac{\gamma t}{2m}} [a(e^{at} + e^{-at}) + \frac{\gamma}{2m}(e^{-at} - e^{at})] C_x(0) + \frac{A}{2am} e^{-\frac{\gamma t}{2m}} \left[ \frac{s_1}{s_1^2 + \Omega_0^2} e^{at} + \frac{s_2}{s_2^2 + \Omega_0^2} e^{-at} \right] + \frac{A}{m} \frac{\left(\Omega^2 - \Omega_0^2\right) \cos(\Omega_0 t) + \frac{\gamma \Omega_0}{m} \sin(\Omega_0 t)}{\left(\Omega^2 - \Omega_0^2\right)^2 + \frac{\gamma}{m}\Omega^2 - \left(\Omega^2 - \Omega_0^2\right)\left(\frac{\gamma}{m}\right)^2}. \tag{A3}$$

Evidently, the oscillatory behavior is provided by the third term of Eq. (A3). The amplitude is modulated by the harmonic potential and the applied periodic signal, whereas the frequency is only related to the external signal, and hence a kind of forced oscillation is obtained.

## APPENDIX B: MONTE CARLO SIMULATION OF THE GLE DRIVEN BY DEBYE-TYPE NOISE

The GLE describing a particle of mass $m$ in a potential reads

$$m\dot{v}(t) = -m \int_0^t \Gamma(t - t_1) v(t_1) dt_1 - U'(x) + F(t). \tag{B1}$$

The key in solving Eq. (B1) with Debye-type noise is through simulations of Debye-type colored noise. As is well known, the main characteristic of Debye-type noise is the noise spectral density

$$\rho(\omega) = \begin{cases} \frac{3\gamma^2}{\omega_s^3} & \omega \leqslant \omega_s, \\ 0 & \text{otherwise} \end{cases} \tag{B2}$$

and the correlation function $\langle F(t)F(0)\rangle = \Gamma(t) = 3\gamma^2 \omega_s^{-3} \sin(\omega_s t) t^{-1}$. In the calculation, we have for convenience set $m = 1$ and $k_B T = 1$. In $\omega$-Fourier space, the noise correlation function reads

$$\langle F(\omega)F(\omega')\rangle = 2\pi \Gamma(\omega)\delta(\omega + \omega'), \tag{B3}$$

where $F(\omega)$ and $\Gamma(\omega)$ denote the Fourier transforms of $F(t)$ and $\Gamma(t)$, respectively. Next, we discretize time into intervals of size $\Delta t$; the Fourier space may also be discretized, the discretization of Eq. (B3) yielding

$$\langle F(\omega_\mu)F(\omega_\nu)\rangle = \Gamma(\omega_\mu) N \Delta t \delta_{\mu+\nu,0}. \tag{B4}$$

We then obtain, in Fourier space, noise spectrum

$$F(\omega_\mu) = \sqrt{N \Delta t \Gamma(\omega_\mu)} \alpha_\mu, \quad \mu = 1, \ldots, N-1, \qquad F(\omega_0) = \Gamma(\omega_N), \tag{B5}$$

where $\alpha_\mu$ are Gaussian random numbers with zero mean and correlation $\langle \alpha_\mu \alpha_\nu \rangle = \delta_{\mu,-\nu}$. Therefore, $\alpha_\mu$ can be expressed as

$$\alpha_0 = a_0 \quad \alpha_\mu = \frac{1}{\sqrt{2}}(a_\mu + i b_\mu), \tag{B6}$$

where $a_\mu$ and $b_\mu$ denote normal Gaussian random numbers, and $i$ denotes the imaginary unit. Finally, the discrete noise sequences $F(\omega_\mu)$ in Fourier space are obtained, and $F(t)$ can also be calculated through the inverse Fourier transform.

As noise sequences have been given, the second-order stochastic Runge-Kutta method [47] is appropriate to solve the GLE driven by Debye-type noise. For validation, we compared the noise correlation function evaluated numerically from $\Gamma(t_i) = \frac{1}{N_t} \sum_{j=0}^{N_t} \langle F(t_i + j\Delta t) F(t_i)\rangle$ with its theoretical value $\Gamma(t)$ (Fig. 8). The two results are in agreement.


[1] P. Debye, Zur Theorie der spezifischen Wärmen, Ann. Phys. (NY) **39**, 789 (1912).

[2] M. Born Max and K. Huang, *Dynamical Theory of Crystal Lattices* (Clarendon, Oxford, 1954).

[3] L. D. Landau and E. M. Lifshitz, *Statistical Physics*, 3rd ed. (Butterworth, Oxford, 1980), Part 1.

[4] D. A. Garanin, Extended Debye model for molecular magnets, Phys. Rev. B **78**, 020405(R) (2008).

[5] Z. Chen, Z. Wei, Y. Chen, and C. Dames, Anisotropic Debye model for the thermal boundary conductance, Phys. Rev. B **87**, 125426 (2013).

[6] M. Paoluzzi, L. Angelani, G. Parisi, and G. Ruocco, Relation between Heterogeneous Frozen Regions in Supercooled Liquids and Non-Debye Spectrum in the Corresponding Glasses, Phys. Rev. Lett. **123**, 155502 (2019).

[7] Kittel, *Introduction to Solid State Physics* (Wiley, New York, 1976).

[8] G. Reményi, S. Sahling, K. Biljaković, D. Starešinić, J.-C. Lasjaunias, J. E. Lorenzo, P. Monceau, and A. Cano, Incommensurate Systems as Model Compounds for Disorder Revealing Low-Temperature Glasslike Behavior, Phys. Rev. Lett. **114**, 195502 (2015).

[9] M. Baity-Jesi, V. Martín-Mayor, G. Parisi, and S. Perez-Gaviro, Soft Modes, Localization, and Two-Level Systems in Spin Glasses, Phys. Rev. Lett. **115**, 267205 (2015).

[10] S. L. Qiu, F. Apostol, and P. M. Marcus, Low-temperature properties of fcc Al from modified Debye theory, J. Phys. Condens. Matter **19**, 136213 (2007).

[11] G. Shafai, M. A. Ortigoza, and T. S. Rahman, Vibrations of Au 13 and FeAu 12 nanoparticles and the limits of the Debye temperature concept, J. Phys. Condens. Matter **24**, 104026 (2012).

[12] R. Silbey and R. W. Munn, General theory of electronic transport in molecular crystals. I. Local linear electron-phonon coupling, J. Chem. Phys. **72**, 2763 (1980).

[13] R. Zwanzig, Nonlinear generalized Langevin equations, J. Stat. Phys. **9**, 215 (1973).

[14] J. D. Bao, P. Hänggi, and Y. Z. Zhuo, Non-Markovian Brownian dynamics and nonergodicity, Phys. Rev. E **72**, 061107 (2005).

[15] P. Hänggi, G. L. Ingold, and P. Talkner, Finite quantum dissipation: The challenge of obtaining specific heat, New. J. Phys. **10**, 115008 (2008).

[16] M. H. Lee, Ergodic Theory, Infinite Products, and Long Time Behavior in Hermitian Models, Phys. Rev. Lett. **87**, 250601 (2001).

[17] L. C. Lapas, R. Morgado, M. H. Vainstein, J. M. Rubí, and F. A. Oliveira, Khinchin Theorem and Anomalous Diffusion, Phys. Rev. Lett. **101**, 230602 (2008).

[18] D. Thirumalai, R. D. Mountain, and T. R. Kirkpatrick, Ergodic behavior in supercooled liquids and in glasses, Phys. Rev. A **39**, 3563 (1989).

[19] J. Lloyd, L. Rondoni, and G. P. Morriss, Breakdown of ergodic behavior in the Lorentz gas, Phys. Rev. E **50**, 3416 (1994).

[20] F. Bardou, J. P. Bouchaud, O. Emile, A. Aspect, and C. Cohen-Tannoudji, Subrecoil Laser Cooling and Lévy Flights, Phys. Rev. Lett. **72**, 203 (1994).

[21] W. Buijsman, V. Gritsev, and R. Sprik, Nonergodicity in the Anisotropic Dicke Model, Phys. Rev. Lett. **118**, 080601 (2017).

[22] Y. Wang, X. B. Ren, K. Otsuka, and A. Saxena, Evidence for broken ergodicity in strain glass, Phys. Rev. B **76**, 132201 (2007).

[23] E. Lutz, Power-Law Tail Distributions and Nonergodicity, Phys. Rev. Lett. **93**, 190602 (2004).

[24] A. Dechant, E. Lutz, D. A. Kessler, and E. Barkai, Fluctuations of Time Averages for Langevin Dynamics in a Binding Force Field, Phys. Rev. Lett. **107**, 240603 (2011).

[25] A. I. Khinchin, *Mathematical Foundations of Statistical Mechanics* (Dover, New York, 1949).

[26] M. H. Lee, Birkhoff's Theorem, Many-Body Response Function, and the Ergodic Condition, Phys. Rev. Lett. **98**, 110403 (2007).

[27] N. W. N. W. McLachlan, *Laplace Transforms and their Applications to Differential Equations* (Dover, New York, 2014).

[28] R. M. S. Ferreira, M. V. S. Santos, C. C. Donato, J. S. Andrade, and F. A. Oliveira, Analytical results for long-time behavior in anomalous diffusion, Phys. Rev. E **86**, 021121 (2012).

[29] H. K. Shin, B. Choi, P. Talkner, and E. K. Lee, Normal versus anomalous self-diffusion in two-dimensional fluids: Memory function approach and generalized asymptotic Einstein relation, J. Chem. Phys. **141**, 214112 (2014).

[30] Q. Qiu, X.-Y. Shi, and J.-D. Bao, Mixed nonergodicity of a forced system and its non-stationary strength, Europhys. Lett **128**, 20005 (2019).

[31] H. Mori, Transport, collective motion, and brownian motion, Prog. Theor. Phys. **33**, 423 (1965).

[32] S. A. Adelman and J. D. Doll, Generalized Langevin equation approach for atom/solid surface scattering: General formulation for classical scattering off harmonic solids, J. Chem. Phys. **64**, 2375 (1976).

[33] F. Morgado, F. A. Oliveira, G. G. Batrouni, and A. Hansen, Relation between Anomalous and Normal Diffusion in Systems with Memory, Phys. Rev. Lett. **89**, 100601 (2002).

[34] J. D. Bao, Non-Markovian two-time correlation dynamics and nonergodicity, J. Stat. Phys. **168**, 561 (2017).

[35] M. H. Lee, Can the Velocity Autocorrelation Function Decay Exponentially? Phys. Rev. Lett. **51**, 1227 (1983).

[36] K. Lü and J. B. Bao, Numerical simulation of generalized Langevin equation with arbitrary correlated noise, Phys. Rev. E **72**, 067701 (2005).

[37] A. Papoulis, *Probability, Random Variable, and Stochastic Process* (McGraw-Hill, New York, 1989).

[38] H. Risken, *The Fokker-Planck Equation* (Springer-Verlag, Berlin, 1989).

[39] M. Franaszek, Cutoff frequency of experimentally generated noise: A Melnikov approach, Phys. Rev. E **54**, 3003 (1996).

[40] R. N. Mantegna and B. Spagnolo, Stochastic resonance in a tunnel diode in the presence of white or coloured noise, Nuovo. Cimento. D **17**, 873 (1995).

[41] L. Fronzoni, *Noise in Nonlinear Dynamical Systems* (Cambridge University, Cambridge, England, 1989).

[42] A. D. Viñales and M. A. Despósito, Anomalous diffusion: Exact solution of the generalized Langevin equation for harmonically bounded particle, Phys. Rev. E **73**, 016111 (2006).

[43] F. Guinea, V. Hakim, and A. Muramatsu, Diffusion and Localization of a Particle in a Periodic Potential Coupled to a Dissipative Environment, Phys. Rev. Lett. **54**, 263 (1985).

[44] L. R. M. Wilson and K. I. Hopcraft, Periodicity in the autocorrelation function as a mechanism for regularly occurring zero crossings or extreme values of a Gaussian process, Phys. Rev. E **96**, 062129 (2017).

[45] P. Hänggi and P. Jung, Colored noise in dynamical systems, Adv. Chem. Phys. **89**, 239 (1995).

[46] J. D. Bao and Y. Z. Zhuo, Ballistic Diffusion Induced by a Thermal Broadband Noise, Phys. Rev. Lett. **91**, 138104 (2003).

[47] R. L. Honeycutt, Stochastic Runge-Kutta algorithms. I. White noise, Phys. Rev. A. **45**, 600 (1992).